GPO PRICE $ ________

CFSTI PRICE(S) $ 1.00

Hard copy (HC) ________

Microfiche (MF) .50

ff 653 July 65

FACILITY FORM 602

N66 37683	
(ACCESSION NUMBER)	(THRU)
27	1
(PAGES)	(CODE)
TMX-1292	22
(NASA CR OR TMX OR AD NUMBER)	(CATEGORY)

NASA TM X-1292

ANALYSIS OF CONDENSING PRESSURE CONTROL FOR SNAP-8 SYSTEM

By Donald R. Packe, Andrew A. Schoenberg,
Kent S. Jefferies, and Roy C. Tew

Lewis Research Center
Cleveland, Ohio

NATIONAL AERONAUTICS AND SPACE ADMINISTRATION

For sale by the Clearinghouse for Federal Scientific and Technical Information
Springfield, Virginia 22151 – Price $1.00

ANALYSIS OF CONDENSING PRESSURE CONTROL FOR SNAP-8 SYSTEM

by Donald R. Packe, Andrew A. Schoenberg,
Kent S. Jefferies, and Roy C. Tew

Lewis Research Center

SUMMARY

The expected variations of condensing pressure and methods for controlling these variations in the SNAP-8 Rankine space power system were investigated. The effects of environmental disturbances and component degradation on the system operation were studied by means of a steady-state digital computer simulation of the heat-rejection loop and condenser. This study indicated that condensing pressure control may be required to prevent the pressure from exceeding the maximum permitted turbine back pressure required to achieve rated power output or from going below the value necessary to prevent cavitation of the power loop pump. Several methods of controlling condensing pressure were investigated also by steady-state simulation on the digital computer. The most promising forms of control were found to be condenser coolant bypass flow control and condensate inventory control by an accumulator. The dynamic characteristics of these two forms were studied in detail, both by computer simulation and transfer function analysis techniques.

These studies led to the conclusion that for the expected space environment and for present system compatibility including ground testing, the condenser coolant bypass flow control is the best form of pressure control. This method of control is flexible in that its development may parallel system development on a noninterference basis and at a later date may be severed from the program if tests indicate that it is not needed. This feedback control system is expected to be stable, to operate effectively under acceleration conditions, and to maintain condensing pressure well within specified limits under all expected disturbances within the anticipated system flight envelope.

INTRODUCTION

The operating point of a Rankine cycle space power system, such as SNAP-8, may vary from the design value because of changes in the environment of the system, activity of the various controllers, degradation in the system components, and manufacturing tolerances. In spite of this variation a minimum turbine power must be maintained, and power loop pump cavitation must be avoided. This latter requirement is critical because the pump must operate for the duration of the system life of 10 000 hours. Satisfactory operation with respect to these requirements depends on the condenser performance in that too high a condensing pressure will degrade turbine power while too low a pressure may reduce the pump suction head below the level required for prevention of cavitation. This latter condition is especially critical in zero-gravity conditions since pump suction is entirely dependent on condensing pressure and subcooling. The problem of estimating the variations in condensing pressure and if necessary of controlling the pressure within specified limits is considered in this report. Additional work on this problem has been undertaken by the SNAP-8 contractor.

The configuration for the SNAP-8 system, which consists basically of three heat-transfer loops, is analyzed. The first loop transfers heat from the reactor to the mercury boiler by circulating liquid NaK, a eutectic mixture of sodium and potassium. The second loop (power loop) represents the actual Rankine cycle employing mercury as the working fluid. After passing through the turbine, the mercury vapor is condensed and subcooled in a counterflow tube-in-shell condenser. The third loop (heat-rejection loop), which like the first circulates liquid NaK, transfers the heat from the condenser into the radiator for dissipation into space.

The operation of the condenser depends on the heat-rejection loop flow rate and the radiator characteristics, as well as the variables set by power loop operation: namely, power loop flow rate, condenser inlet quality, and condensate inventory inside the condenser tubes. The latter three variables are set primarily by the pump, boiler, and turbine-inlet-nozzle subsystem interacting with the primary loop with negligible influence from the condenser. This lack of influence is due basically to the high value of the ratio of boiler operating pressures to condenser operating pressures (thus minimizing the influence of changes of condensing pressure on the boiler) and to the large amount of boiler inlet subcooling (thus minimizing temperature feedback effects). While inadequate heat-rejection loop performance could cause pump cavitation with a profound influence on boiler operation through reduction in system flow, this problem is precisely what any control system studied herein seeks to prevent; thus, this interaction would not occur in a properly controlled system. Because of this negligible influence of the condenser variables (during proper system operation) on the boiler operation, the condenser and its interaction with the heat rejection loop can conveniently and appropriately be studied separately from the remainder of the system. The boiler output power and flow rates thus serve as independent input variables to the condenser.

In order to analyze the performance of the condenser in the heat-rejection loop, the various interacting components of this SNAP-8 subsystem were simulated on a digital computer. A detailed steady-state simulation of the condenser and radiator was used to determine the sensitivities of the condensing pressure to various system disturbances, such as changes in mercury inlet quality, mercury flow, heat-rejection loop (NaK) flow, condensate inventory, variations in space sink temperature, and degradation and uncertainties in emissivity of the radiator. This program was also used to evaluate the effectiveness in the steady state of various modes of condensing pressure control. An additional digital program incorporating the proposed control modes and the dynamic properties of the components was developed to study the transient behavior of the controlled condenser and heat-rejection loop.

The analysis was divided into three parts. In the first part the expected steady-state variations in condensing pressure were investigated to determine under what conditions pressure control was needed. In the second part the best methods of pressure control were established. In the last part the dynamic characteristics of the more promising modes of control were investigated and evaluated.

SYMBOLS

A_c	flow cross-sectional area of condenser tubes, $n_t \pi D^2/4$
a	acceleration component along the condenser axis
C_N	specific heat of condenser coolant (NaK)
D	diameter of tube
g	acceleration of gravity
I_N	condenser coolant inventory in condensing region
K_c	gain of coolant flow controller (percent flow/^{O}F)
K_D	gain of dead-band controller representing the rate of change of coolant flow (percent flow/sec)
K_g	gain constant of pressure at inlet of accumulator to axial acceleration
K_p	gain constant proportional to mercury liquid flow resistance, $\frac{\partial w_L}{\partial P_c} \frac{1}{w_L}$
K_{sat}	slope of mercury saturation curve at SNAP-8 operating point, 0.15 psi/^{O}R
$K_T G_T(s)$	transfer function of transducer and control valve for condenser coolant bypass control system

K_w	gain constant of condensing temperature to coolant flow, $\frac{\overline{Q}}{\overline{w}_N C_N} \frac{1}{\left(1 - e^{-NTU}\right)} - K_1(1 - \beta_w)$
K_1	gain constant of condensing temperature to inventory, $\frac{\overline{Q}}{w_N C_N} \frac{NTU\ e^{-NTU}}{\left(1 - e^{-NTU}\right)^2}$
L_c	condensing length
L_L	length of liquid column inside condenser tube
n_t	number of condensing tubes
NTU	number of transfer units of condensing region, $\int_0^{L_c} \frac{n_t U \pi D\ dL_c}{w_N C_N}$
P_A	accumulator pressure
ΔP_a	pressure disturbance at accumulator due to acceleration head on condenser
P_c	condensing pressure
Q	thermal power into the condenser
S_c	solar constant
s	Laplace operator
T_c	condensing temperature
$T_{N,i}$	condenser coolant inlet temperature
T_s	space sink temperature
U	overall coefficient of heat transfer in condensing region
u	disturbance variable on condensing temperature due to variation of mercury inlet flow and/or coolant inlet temperature
V_c	volume of condensing region
W_c	weight of condensate in condenser
w_L	mercury liquid flow out of the condenser
w_M	mercury vapor flow into the condenser
w_N	condenser coolant (NaK) flow rate
X	quality of mercury vapor at condenser inlet
α	absorptivity of radiator

β_w dimensionless sensitivity of U to changes in coolant flow, $\frac{\partial U}{\partial w_N} \frac{\bar{w}_N}{\bar{U}}$

ϵ emissivity of radiator surface

ρ_L mercury liquid density

τ_a time constant of condenser, $\frac{\tau_b}{1 + NTU}$

τ_b dwell time of coolant in condensing region

τ_p time constant proportional to liquid column inertia, $\frac{L_L \bar{w}_M K_p}{g A_c}$

τ_w time constant of condensing temperature to coolant flow rate, $\approx \tau_b$

τ_θ mercury liquid fill time of condensing region

ω circular frequency, rad/sec

Superscript:

$(\bar{\ })$ reference value of a variable indicated by a bar above the symbol of the variable; example, $\bar{w}_N$

INVESTIGATION OF NEED FOR CONTROL

Before the need for control can be determined, the sensitivity of the condensing pressure to expected changes in the environment and component characteristics of the system must be established, and the magnitude of these changes must be estimated. If the range of condensing pressure resulting from these changes exceeds preestablished limits, some form of control is needed.

Sensitivity of Condensing Pressure

The results presented in this section were determined with a combined condenser and cylindrical radiator steady-state simulation on a digital computer. The mathematical models for this simulation consisted of a closed form solution of an idealized condensing process and an iterative set of equations representing the radiator. With this combination, several perturbations were studied to determine the sensitivity of condensing pres-

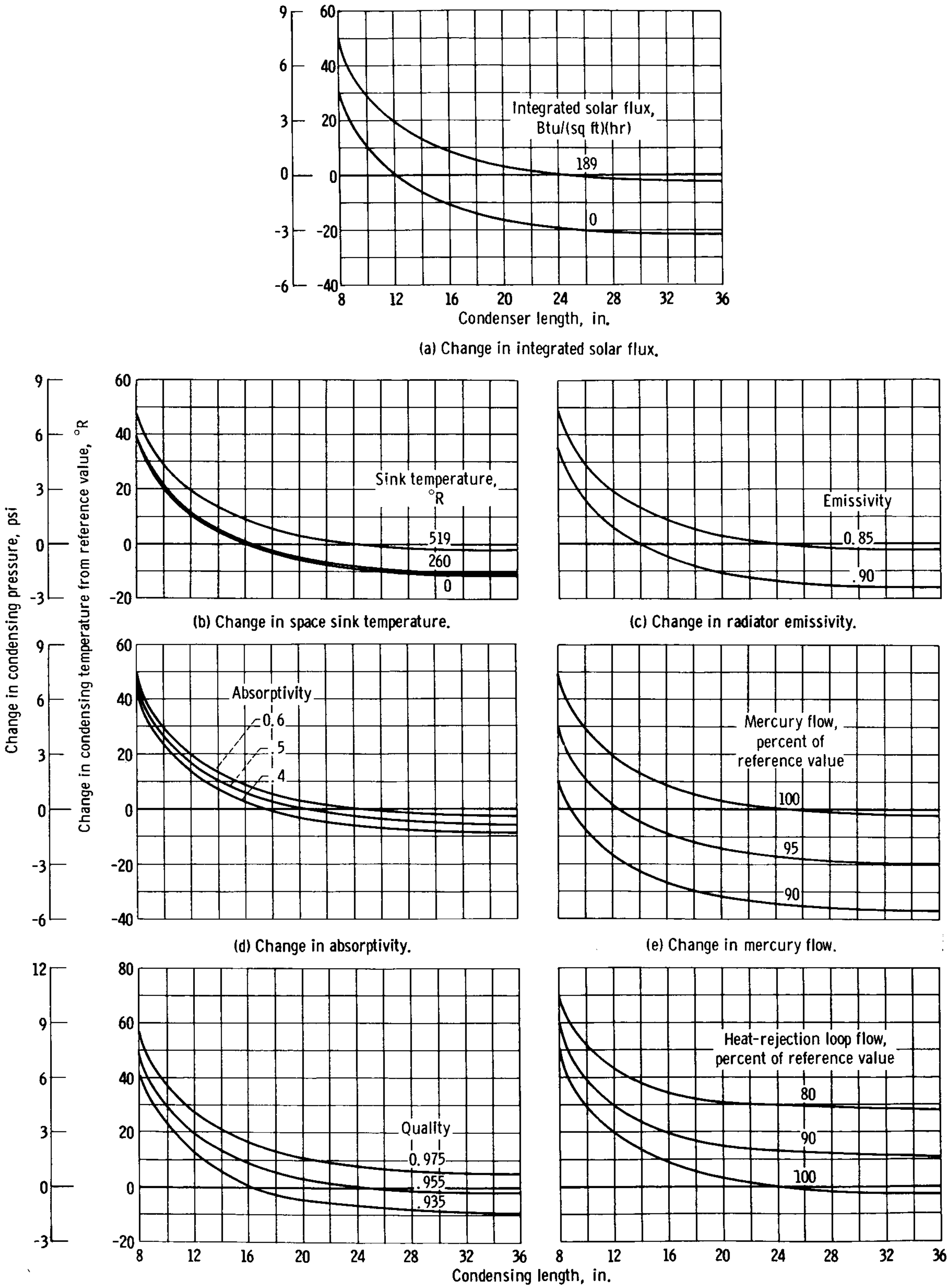

(a) Change in integrated solar flux.

(b) Change in space sink temperature.

(c) Change in radiator emissivity.

(d) Change in absorptivity.

(e) Change in mercury flow.

(f) Change in mercury vapor quality.

(g) Change in heat-rejection loop flow.

Figure 1. - Shift in condensing temperature as function of condensing length due to changes in variables.

TABLE I. - REFERENCE VALUES OF VARIABLES USED FOR SIMULATION

[These numerical values are not necessarily the present design values of SNAP-8.]

Variable	Reference value
Mercury flow, lb/hr	9800
Vapor inlet quality	0.955
Condensing length, in.	25
Heat-rejection loop (NaK) flow, lb/hr	34 700
Solar flux integrated over cylindrical radiator, Btu/(ft^2)(hr)	[a]189
Emissivity	0.85
Absorptivity	0.6
Sink temperature, $^{\circ}R$	[b]519

[a]Direct plus albedo.
[b]Near-earth orbit.

sure. The perturbations were made about the reference values of the variables listed in table I. The results are shown in figure 1. The change in condensing temperature was obtained directly from the condenser simulation. For convenience, the corresponding change in the saturation pressure is also shown. The condensing pressure scale was obtained by using the slope of the saturation curve for the working fluid at the design temperature. For the SNAP-8 condenser, the conversion factor 0.15 pound per square inch per $^{\circ}R$ was used.

The sensitivity of condensing pressure to each of the variables except condensing length is obtained from the distance between the curves of condensing temperature against condensing length in each figure. The sensitivity to condensing length variation is indicated simply by the slope of each curve as plotted. For comparison, the following empirical formula was derived from these figures to show the sensitivities in dimensionless numerical form:

$$\Delta P_c = K_{sat}\left(20\frac{\Delta S_c}{\overline{S}_c} + 350\frac{\Delta w_M}{\overline{w}_M} + 350\frac{\Delta X}{\overline{X}} - 280\frac{\Delta \epsilon}{\overline{\epsilon}} + 18\frac{\Delta \alpha}{\overline{\alpha}} + 50\frac{\Delta T_s}{\overline{T}_s} - 15\frac{\Delta L_c}{\overline{L}_c} - 150\frac{\Delta w_N}{\overline{w}_N}\right) \quad (1)$$

These sensitivities were evaluated at the reference values given in table I. The equation and the figures show that the highest sensitivities are for mercury flow rate, inlet quality, radiator emissivity, and heat-rejection loop flow rate. Note, however, that although the sensitivity to solar flux is approximately an order of magnitude less than the four mentioned previously, the magnitude of the potential perturbation (sun-shade orbit) is so large that a substantial disturbance occurs in the system. The sensitivity to condensing length is low for the reference condition. The increase of this sensitivity, upon which one of the control forms depends, will be discussed in the section Condenser Inventory Control of Pressure.

Estimated Variations in Condensing Pressure

After the sensitivities of the system to various disturbances are established, the mag-

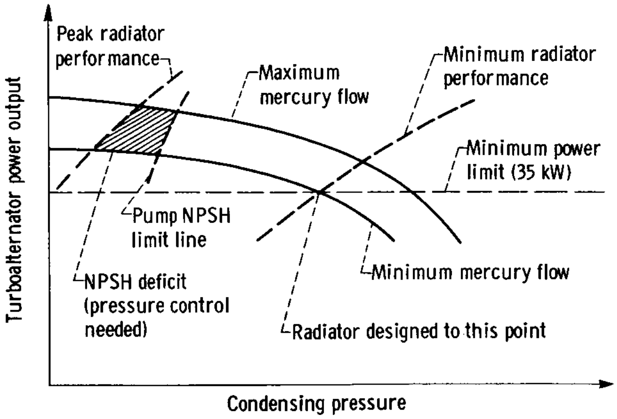

Figure 2. - Effect of condensing pressure variations on turboalternator output and NPSH illustrating area where pressure control is needed. (NPSH, net positive suction head.)

nitude of these disturbances must be estimated to determine the variations in condensing pressure that can be expected. The magnitudes of the disturbances are very difficult to predict accurately because they generally depend on such factors as pump degradation, system controller actions, changes in the radiator surface condition during 10 000 hours of operation, as well as environmental disturbances to the system, such as sun-shade transitions. Estimates of the disturbance magnitudes, however, indicate that the variation in condensing pressure may be large enough to be a problem. The general problem is illustrated in figure 2. The two solid curves represent the predicted variation of the turboalternator electric power output as a function of condensing pressure (turbine back pressure) for the highest and lowest anticipated power loop flow rates. The two dashed curves indicate the condensing pressure for various mercury flow rates for the extremes in radiator performance, both in terms of environmental perturbations and degradation. Radiator performance is most critical when the mercury flow is minimum and the condensing pressure is the maximum possible with the minimum mercury flow rate. The radiator has to be designed with enough capacity so that the condensing pressure is low enough to allow the turboalternator to supply the minimum power requirement (35 kW for SNAP-8) at this condition.

With the radiator capacity designed for the critical point, the possibility exists that when the radiator environment and power level change so as to reduce the condensing pressure to its lowest value, as may occur in a transition from sun to shade when the mercury flow is at a minimum, a net positive suction head deficit may be created, and cavitation of the pump may result. The prevention of this type of operation requires some form of pressure control. Whether these conditions will actually occur is very difficult to establish without actual system testing and the definition of a mission. The need for a pressure control may be diminished by operation in a gravity environment (e.g., a moon-base powerplant) where pump net positive suction head is aided by gravity head. In the event, however, that pressure control is required, it is desirable to have an effective controller ready to include in the system. What type of control this should be is considered next.

STEADY-STATE EVALUATION OF VARIOUS FORMS OF CONTROL

Five control modes (composite shown in fig. 3) were studied to determine their relative advantages, disadvantages, and control sensitivities. The first four are all forms of flow control in the heat-rejection loop. The fifth is control of the condenser condensate inventory.

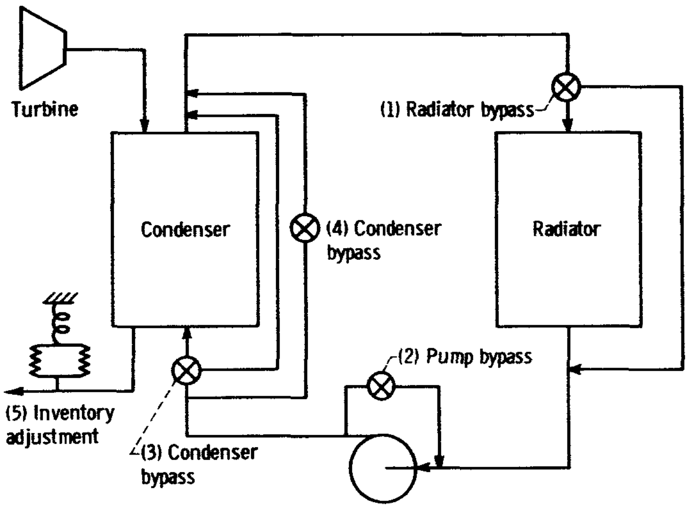

Figure 3. - Control modes studied.

The first form studied was radiator bypass, which utilized a three-way valve, diverting some of the flow around the radiator. In this study the total loop flow (other than through the radiator) is assumed to remain constant. The second form was a pump bypass in which some of the flow is passed around the pump, and thus the flow through the condenser and radiator is changed. This form could also utilize a throttling valve or a diverting three-way valve around the pump. The third form of control studied was the condenser bypass. Again the three-way configuration was used to maintain a constant total system flow. The fourth configuration utilized a single valve in a bypass leg around the condenser. In this form of condenser bypass the loop flow changed because of the reduction of pump load (e.g., when the bypass valve was opened, the total system flow would increase slightly). The fifth control system studied was an inventory adjusting mechanism taking the form of an accumulator to shift the mercury inventory into and out of the condenser in order to maintain condenser pressure at a constant level.

Condenser Coolant Flow Controls

The steady-state sensitivities of the first four forms of control are indicated in figure 4. A comparison is made in figure 5 of the resultant change of condensing tempera-

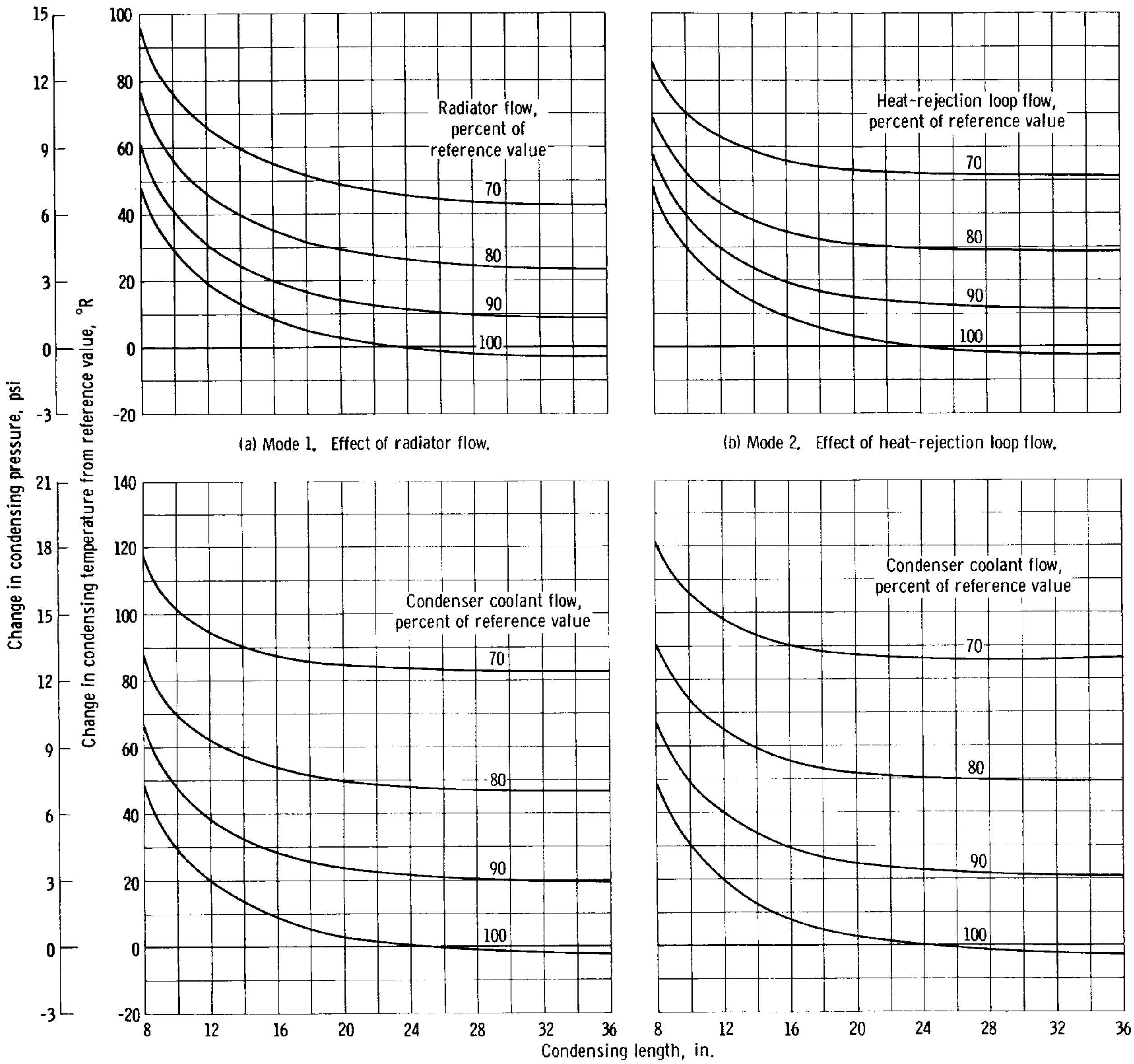

(a) Mode 1. Effect of radiator flow.

(b) Mode 2. Effect of heat-rejection loop flow.

(c) Mode 3. Effect of condenser coolant flow using 3-way control valve.

(d) Mode 4. Effect of condenser coolant flow using bypass control valve.

Figure 4. - Effects of various control modes on characteristic curve of condensing temperature as a function of condensing length.

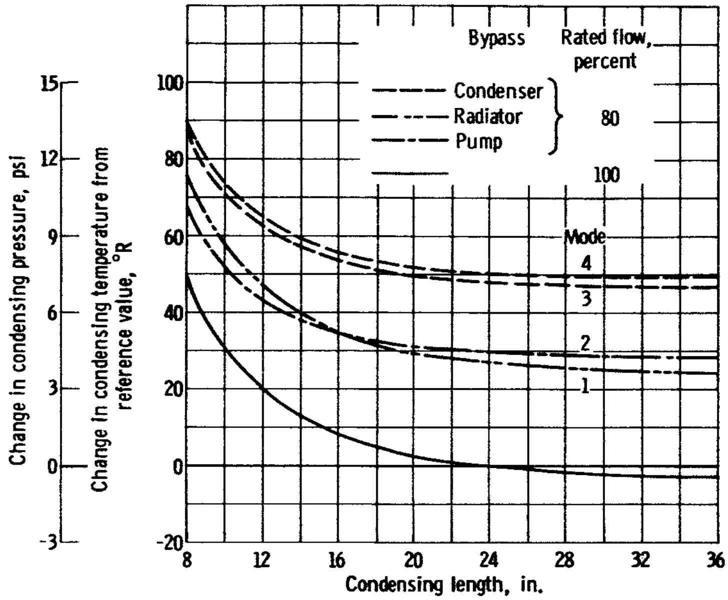

Figure 5. - Comparison of effectiveness of four modes of condenser coolant flow control in shifting characteristic curve of condensing temperature as a function of condensing length.

ture to a 20-percent change of flow for each of the four modes of control. This figure indicates that the condenser bypasses (modes 3 and 4) are approximately twice as effective as the other two flow control modes. The choice of either mode 3 or 4 becomes essentially arbitrary, at least with respect to control sensitivity. One deciding factor, however, could be the control range desired. If the controller must handle large amplitude disturbances or large shifts in system operating point, the simple bypass valve configuration of mode 4 should not be used because it would require a bypass leg of low pressure drop design compared with condenser pressure drop so that a substantial portion of the flow could bypass the condenser. This design could be weighty and cumbersome. Under these circumstances, mode 3 would probably be preferred. For convenience, further discussions of condenser coolant bypass control will be confined to mode 3. It is felt that the results will be equally applicable to mode 4.

In order to understand the control sensitivity from another viewpoint, figure 6 was prepared (a cross plot of fig. 4(c)) to show directly the change of condensing temperature for a change of condenser flow rate for mode 3 control. The approximate slope of these lines is 2.5° F per percent change of coolant flow.

An effect that was not a part of the computer simulation but which was noted from experimental data is shown in figure 7, in which the heat-transfer coefficient is plotted as a function of condenser coolant flow rate. The figure indicates that, as coolant flow rate increases, the heat-transfer coefficient also tends to increase. This characteristic tends to favor condensing pressure control by means of condenser coolant flow rate; that is, an

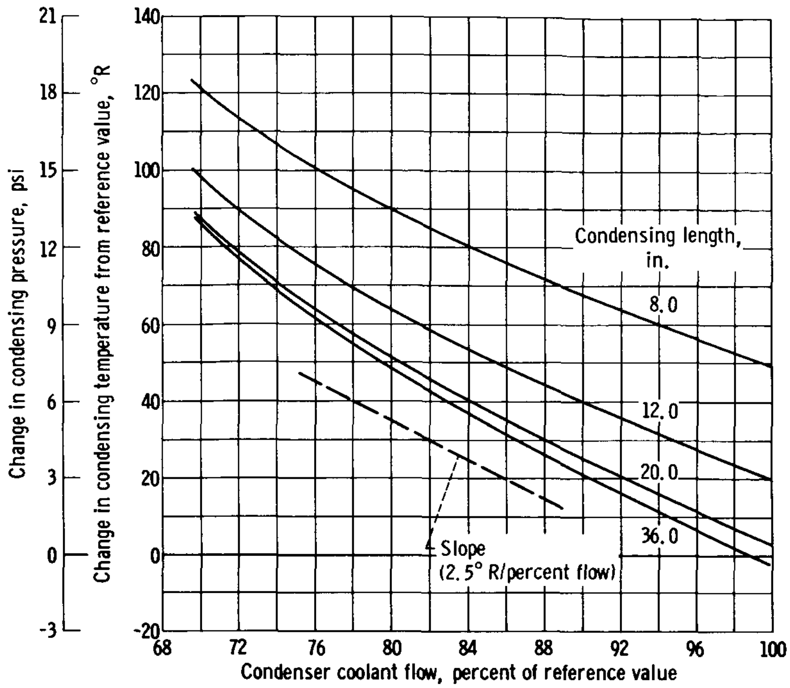

Figure 6. - Change in condensing temperature as function of condenser coolant flow for several condensing lengths. Mode 3 control.

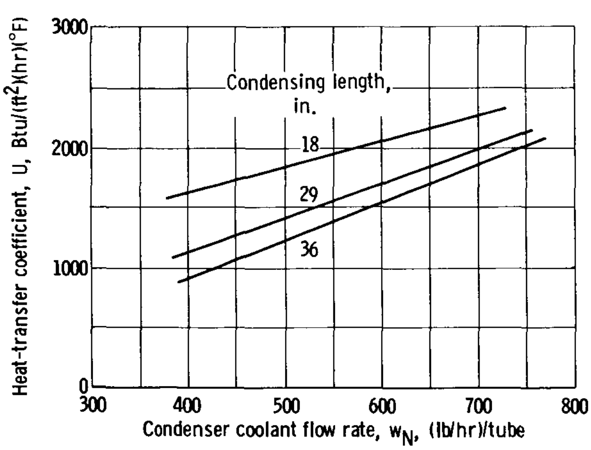

Figure 7. - Best fit curves of heat-transfer coefficient as function of condenser coolant flow rate for SNAP-8 single-tube experimental data.

increase of coolant flow rate for the purpose of reducing condenser pressure would be aided by the accompanying increase of heat-transfer coefficient. In the same manner, a decrease of coolant flow for the purpose of increasing condenser pressure would be aided by the resulting decrease of heat-transfer coefficient.

The other condensing pressure control to be considered is based on changing the condenser liquid inventory. This method, mode 5, is examined next.

Condenser Inventory Control of Pressure

Condensing pressure (temperature) may be controlled by varying the length available for condensing, or in other words, by varying the condenser liquid inventory. This is

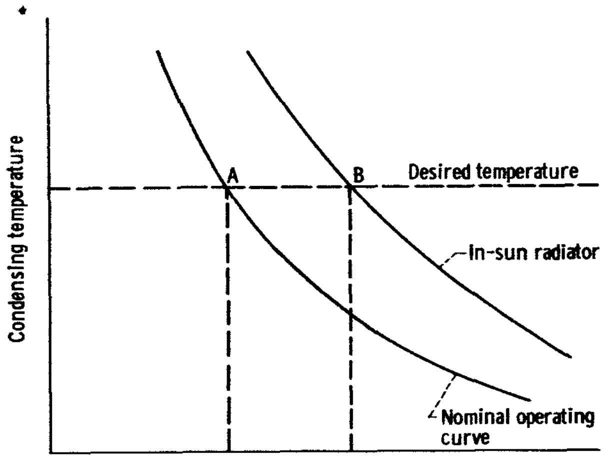

Figure 8. - Condenser temperature (pressure) control by varying condensate inventory.

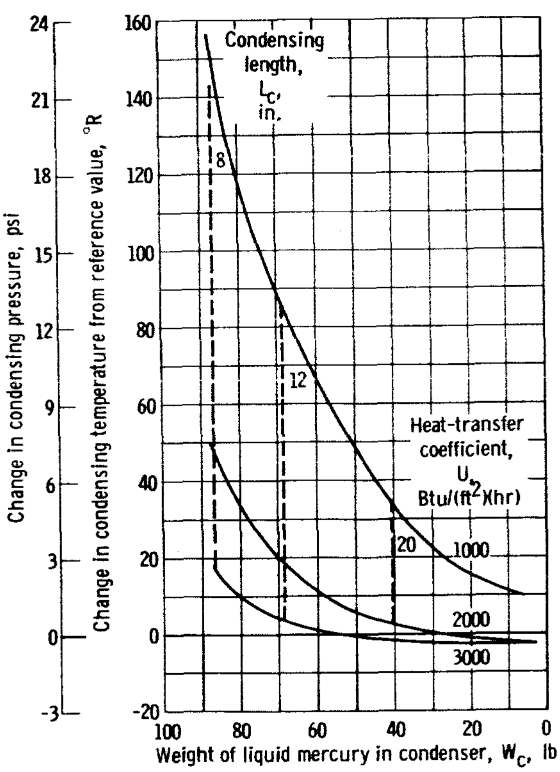

Figure 9. - Change in condensing temperature as function of weight of liquid mercury in condenser for various values of heat-transfer coefficient.

illustrated in figure 8 where a nominal operating curve of condensing temperature against inventory is shown. If the condenser operation is shifted by changed inlet conditions (e.g., the in-sun radiator curve), the condensing temperature may be held constant at the desired value by changing the inventory from A to B.

In order to be effective, the inventory control must operate on the high-slope portion of the temperature-inventory characteristic curve. In addition, from a dynamics point of view, the slope should be sensibly constant over the expected operating range of the control. A counterflow condenser, however, displays an exponential characteristic such as that shown for SNAP-8 in figure 9 rather than the preferred linear one. A study was made to determine whether any redesign of the condenser would improve the exponential characteristic so that it would become a linear characteristic. The three parameters chosen for the study were heat-transfer coefficient, tube diameter, and coolant flow rate. All these parameters appreciably change the sensitivity of condensing temperature to interface position (figs. 9 to 11). These characteristics may be better understood by examining the equations for a theoretical model of the condenser.

An important parameter in heat-exchanger theory is the number of transfer units NTU, which is defined by the following equation:

$$NTU = \int_0^{L_c} \frac{n_t U \pi D \, dL_c}{w_N C_N} \qquad (2)$$

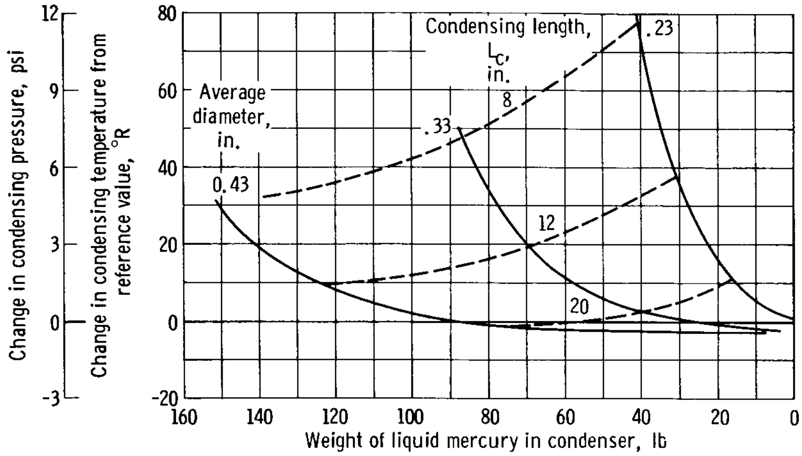

Figure 10. - Change in condensing temperature as function of weight of liquid mercury for various average diameters of tapered tubes.

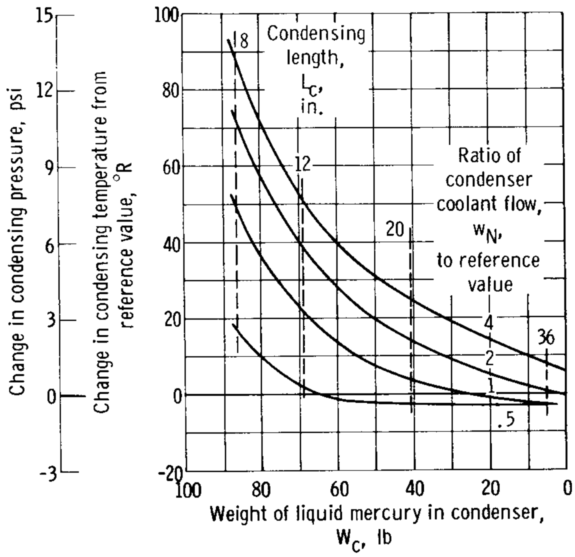

Figure 11. - Change in condensing temperature as function of weight of liquid mercury in condenser for various values of condenser coolant flow. Condenser coolant outlet temperature constant.

where

U	overall local heat-transfer coefficient
πD	heat-transfer area per unit length
w_N	coolant flow rate
C_N	specific heat of coolant
L_c	condensing length
n_t	number of condensing tubes

The number of transfer units enters into the theoretical expression for the condensing temperature T_c as follows. Assuming the heat-transfer coefficient U and condensing temperature T_c constant with length and using an average tube diameter (in the case of tapered condensing tubes) yield the following equation for T_c:

$$T_c = T_{N,i} + \frac{Q}{w_N C_N} \frac{1}{1 - e^{-NTU}} \tag{3}$$

where $NTU = n_t U \pi \overline{D} L_c / w_N C_N$ and Q is the total heat input to the condenser from the power loop. The exponential nature of the curves in figures 9 to 11 is due to the term $1/(1 - e^{-NTU})$. Examination of this term shows that in general a decrease in NTU makes the condensing temperature more sensitive to variations in any of the parameters entering into the expression for NTU. Thus, a condenser with small NTU will be more responsive

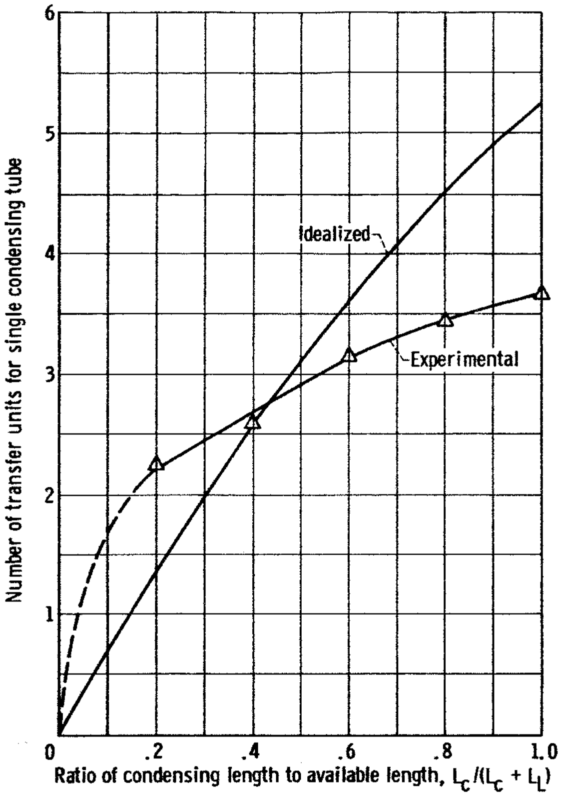

Figure 12. - Comparison of idealized and experimental number of transfer units for single-tube condenser as function of condensing length. Constant overall heat-transfer coefficient, 2000 Btu/(ft^2)(hr)(°F); condenser coolant inlet temperature, 500° F; mercury flow rate, 0.042 pound per second per tube; coolant flow rate, 495 pounds per hour per tube.

to inventory control than one with large NTU. Note, however, that this increase in sensitivity to NTU parameters is accompanied by a similar increase in sensitivity to the disturbance variables (Q, w_N, and $T_{N,i}$) so that a reduction of the NTU may not represent an improvement in overall condenser operation. The preceding considerations apply to the idealized condenser in which the heat-transfer coefficient and condensing temperature do not vary with length. An actual condenser, however, may deviate from this idealized case.

The idealized function of NTU against the condensing length was compared with experimental data obtained for a configuration of the type used for the SNAP-8 condenser. In figure 12 the idealized condenser characteristic with constant heat-transfer coefficient is plotted for U = 2000 Btu/(ft^2)(hr)(^{O}F). The slight curvature of the constant U ideal curve is due to the tapered tubes in the condenser. The other curve shows the experimental data from a single-tube mercury condenser for the same coolant flow rate. These data have an important influence on the characteristic curve of condensing temperature against inventory (fig. 13) where a comparison of the idealized

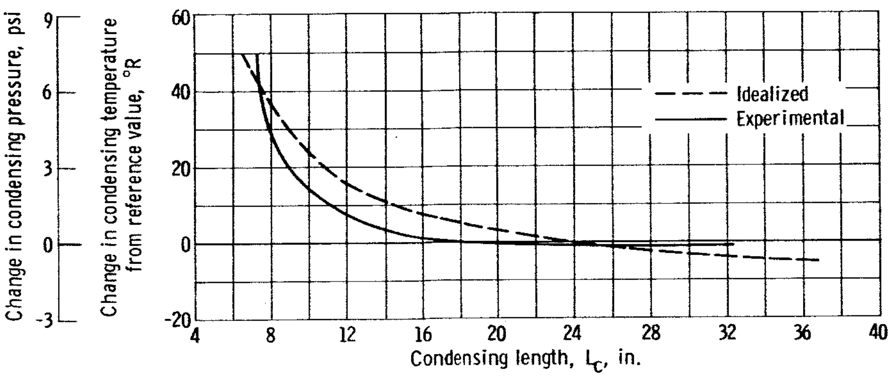

Figure 13. - Experimental and idealized condenser characteristic performance curves showing difference between assumed constant heat-transfer coefficient and actual performance. Assumed constant heat-transfer coefficient, 2000 Btu/(ft^2)(hr)(°F).

curve obtained from equation (3) and experimental data for a single tube is shown. The experimental data indicates a shift from the idealized characteristic that degrades the effectiveness of inventory control. Note that for the flat portion of the curve a change in inventory will not change condensing temperature and, hence, has no control over condensing pressure.

The analysis of the steady-state characteristics of inventory control indicate that the control effectiveness depends on the operating point and the design of the condenser. In general, the low values of NTU were found to be necessary to insure high sensitivity of pressure to inventory changes. The present operating point of the SNAP-8 condenser is not particularly favorable to this type of control. If the condensing length is shortened, however, by starting with a larger liquid-mercury inventory, mode 5 control can be very effective. An important advantage of inventory control with an accumulator is that no pressure or temperature measuring devices are needed since the changes in inventory will be actuated directly by the difference between condensing pressure and the desired pressure as set by the accumulator. Also, any long-term losses of mercury to space will automatically be made up by the excess inventory of the accumulator. Lastly, this control system can be made to respond rapidly to system disturbances. The dynamic characteristics of the control systems are treated in the next section.

DYNAMICS STUDY

The dynamic characteristics of the two most promising modes of control of condensing pressure were investigated: (1) mercury inventory control by means of an accumulator and (2) condenser coolant bypass flow control (mode 3). The study was carried out by (1) a linearized analysis, and (2) a nonlinear dynamic simulation of the condenser and the third loop on a digital computer.

The control systems were evaluated on the basis of the following six criteria:

(1) Stability and damping

(2) Response time

(3) Steady-state offset

(4) Controllable range

(5) Simplicity and reliability

(6) Acceleration sensitivity

The results of the study are summarized in the form of block diagrams derived from the linearized study and in the form of a few typical transient responses to step disturbances in inlet vapor flow rate obtained from the digital computer simulation.

Inventory Control

The dynamic equations describing the condenser and accumulator were linearized about the operating point, and from these equations, the transfer functions of the system were developed. These equations in block-diagram form for the inventory control are given in figure 14. A more complete treatment of the condenser dynamic equations for a

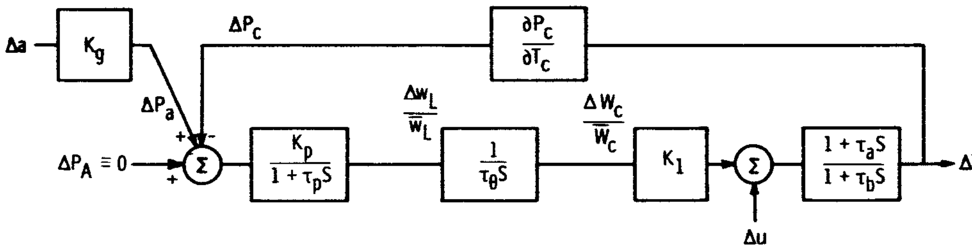

Figure 14. - Block diagram for condensing pressure control using accumulator to adjust condensate coolant inventory.

single tube can be found in reference 1. The first summing element in the block diagram compares the pressure in the accumulator to that in the condenser. Also added at this point is a disturbance proportional to the acceleration of the system. If there is an imbalance in pressure, flow into or out of the condenser results. The flow transfer function has a gain K_p which is inversely proportional to the flow resistance, and a lag term τ_p due to the inertia of the liquid column. The integrated $(1/\tau_\theta S)$ flow produces a net change in condenser inventory $(\Delta W_c/\bar{W}_c)$ and hence in the NTU value of the condenser. This change and the other system disturbance Δu combine to produce a net change in condensing temperature. The Δu input represents the variation due to inlet mercury vapor flow and NaK inlet temperature disturbances. The dynamic element represents the delay in condensing temperature response due to the thermal and transport lag of the NaK coolant in the condenser.

Typical values of the gains and time constants were determined. These approximate values give an indication of the type and range of the dynamics. The formulas and typical values of the gains are as follows:

$$\frac{\partial P_c}{\partial T_c} \approx 0.015 \text{ psia/}^{\circ}\text{R}$$

$$0.5 < K_p \equiv \frac{\partial w_L}{\partial P_c} \frac{1}{\bar{w}_L} < 2 \text{ psi}^{-1}$$

$$K_g \equiv \frac{\rho_L L_L}{g} \approx 0.2 \text{ psi/(ft)(sec}^{-2})$$

$$K_1 \equiv \frac{\overline{Q}}{\overline{w}_N C_N} \frac{NTU\, e^{-NTU}}{\left(1 - e^{-NTU}\right)^2} \approx 50^\circ \text{ R}$$

(The expression for K_1 is the derivative of eq. (3) with respect to L_c, times $\overline{L}_c$.) The time constants are as follows (given in sec):

$$\tau_p \equiv \frac{L_L \overline{w}_M K_p}{g A_c} \approx 0.1$$

$$\tau_\theta \equiv \frac{\rho_L \overline{V}_c}{\overline{w}_M} \approx 33$$

$$\tau_b \equiv \frac{I_N}{\overline{w}_N} \approx 3$$

$$\tau_a \equiv \frac{\tau_b}{1 + NTU} \approx 1$$

The accumulator control system was studied by frequency response techniques based on this linearized model. In these studies the system gain $(K_1 K_p / T_\theta)$ was varied from the value for the reference condition to higher values achievable by shortening the condensing length and altering the condenser design. In general, higher gain occurs in the region of higher slope for the curve of condensing temperature as a function of condensing length. The system responded stably at all gains investigated, and, as expected, the higher gains improved the speed of response. While steady-state offset did not exist in the linearized study because of the inherent integral action of the accumulator, practical limitations, such as friction and nonzero spring constant of the accumulator, would allow small offsets probably no greater than a few percent of design pressure.

The transient response of the condenser with accumulator was studied by means of the digital computer simulation. The transient recovery of the condensing temperature after a step in mercury flow is shown in figure 15. The gain and the speed of response depends on the flow resistance of the liquid column between the vapor-liquid interface and

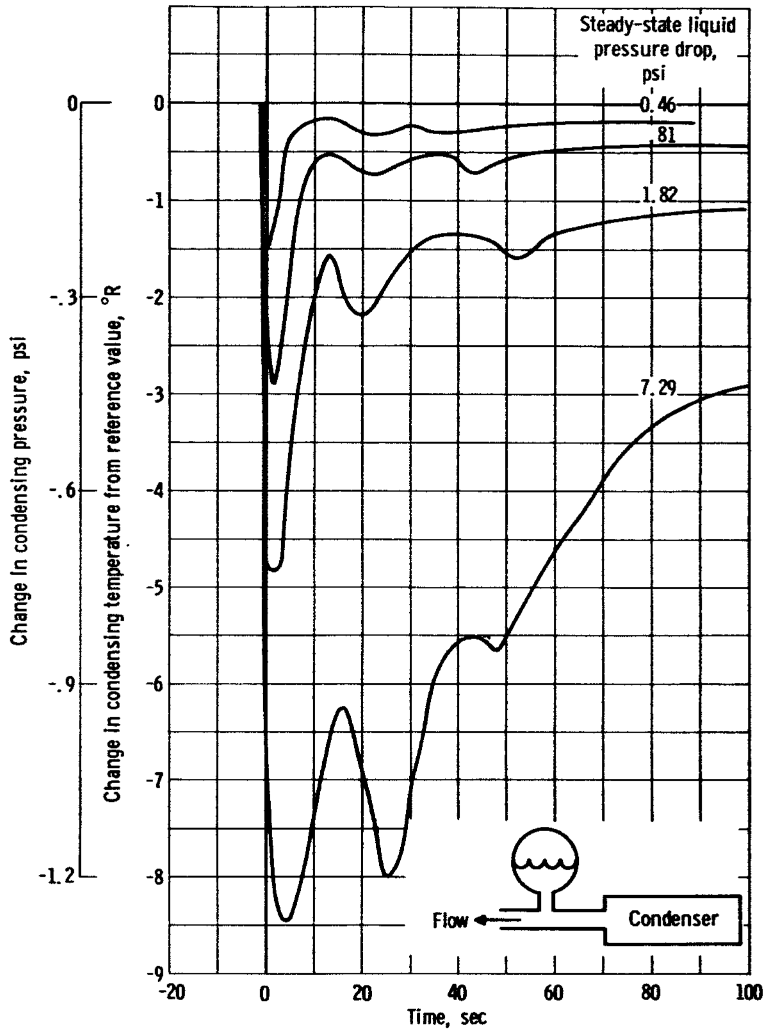

Figure 15. - Transient response of condensing temperature after 5-percent decrease in mercury flow rate from reference value for various values of liquid flow resistance.

the accumulator. For the expected value of liquid pressure drop (0.46 psi) the response is very fast and stable.

The dynamic analysis of the inventory control by means of an accumulator indicates that this form of control has good dynamic characteristics. One serious drawback of this system must, however, be considered: the effect of gravity and acceleration which makes ground testing difficult and when in actual operation makes the controller ineffective during acceleration periods. If instead of a gas or spring loaded accumulator, a positive displacement reservoir is used to adjust inventory, the system becomes insensitive to acceleration. However, a separate sensing device (e.g., a pressure pickup) to command the inventory adjustment and a power source to drive the adjusting mechanism would have to be added; thus the inherent simplicity and rapid response would be reduced compared with the accumulator method.

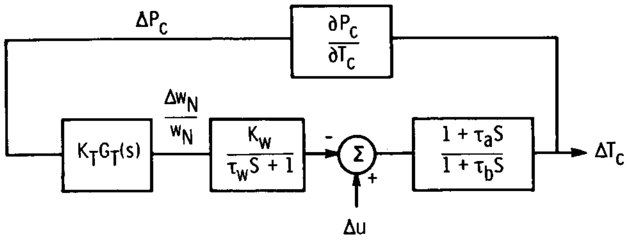

Figure 16. - Block diagram for condensing pressure control using condenser coolant bypass.

Flow Control

The block diagram for the condenser coolant bypass flow control is given in figure 16. The block diagram is similar to that of the inventory control except that the manipulated variable is coolant flow rate rather than mercury inventory. The coolant flow controller dynamics are represented by the term $K_T G_T(s)$. The gain and dynamics of this element will depend on the type of valve and measuring elements used so that its dynamic structure can only be conjectured at this point.

Representative values for the steady-state sensitivities are as follows:

$$K_w = \frac{\bar{Q}}{\bar{w}_N C_N} \frac{1}{(1 - e^{-NTU})} - K_1(1 - \beta_w) \approx 200^\circ R$$

(The expression for K_w is the derivative of eq. (3) with respect to w_N, times $\bar{w}_N$.)

$$0.4 < \beta_w \equiv \frac{\bar{w}_N}{\bar{U}} \frac{\partial U}{\partial w_N} < 0.9$$

$$\tau_w \approx \tau_b$$

$$G_T(s) \approx \frac{1}{1 + \tau_T s}$$

$$\tau_T < 1 \text{ sec}$$

$$K_T = \text{arbitrary gain psi}^{-1}$$

(The constants K_1, τ_a, and τ_b were defined previously.)

With this linearized model the condenser coolant bypass control was studied by using frequency response techniques and by assuming a fast response measuring transducer and controller. The system was stable for all practical values of gain; however, a steady-state error or offset was indicated since no inherent integral action was present in the controller. While offset could be eliminated by adding integral action, it was not deemed

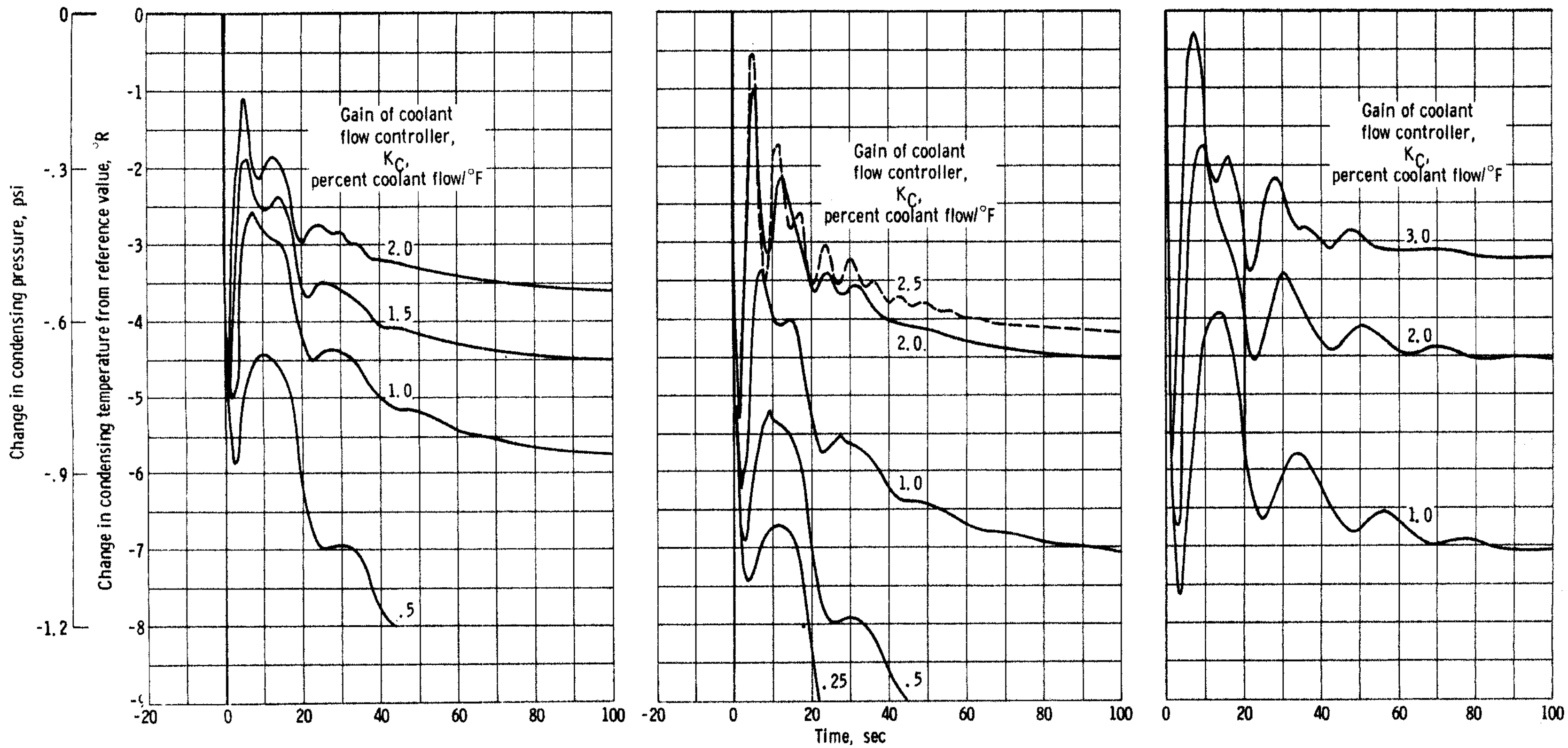

(a) Controller based on condensing temperature measurement with first-order lag of 3 seconds in control action.

(b) Controller based on coolant outlet temperature measurement with first-order lag of 3 seconds in control action.

(c) Controller based on coolant outlet temperature with first-order lag of 10 seconds in control action.

Figure 17. - Effect of gain on condensing temperature response to step decrease in mercury vapor flow for several different condenser coolant bypass controllers.

necessary since the basic function was to control pressure within two rather broad limits; however, the offset was minimized as much as practicable by increasing the proportional gain. This increase, however, may cause less stable or underdamped operation so that careful selection of gain is required for satisfactory response.

The effect of a slow acting controller on the transient responses due to step changes in mercury vapor flow rate and sun-shade perturbations was investigated by using the dynamic digital computer simulation. Figure 17(a) shows the deviation of condensing temperature from the reference value after a 5-percent step decrease in mercury flow for various values of gain. The gain K_c is defined as the percent of change in coolant flow per ^{o}F change in condensing temperature. The controller is assumed to sense the condensing temperature directly without delay. The resultant change in coolant flow was assumed to be a first order lag with a time constant of about 3 seconds. As expected, the offset diminishes with an increase of gain, but the response is slightly more oscillatory. This effect can be seen clearly in figure 17(b) where an additional lag was introduced by controlling the coolant outlet temperature rather than the condensing temperature. Again various values of controller gain were studied. Coolant outlet temperature was studied as a control input since only a small steady-state temperature difference exists between the coolant outlet and the condensing temperatures. Figure 17(c) shows the same transients as those in figure 17(b), but a slower responding controller ($K_T G_T(s)$) was used with a time constant of 10 seconds. As expected, the transient persists for a longer time,

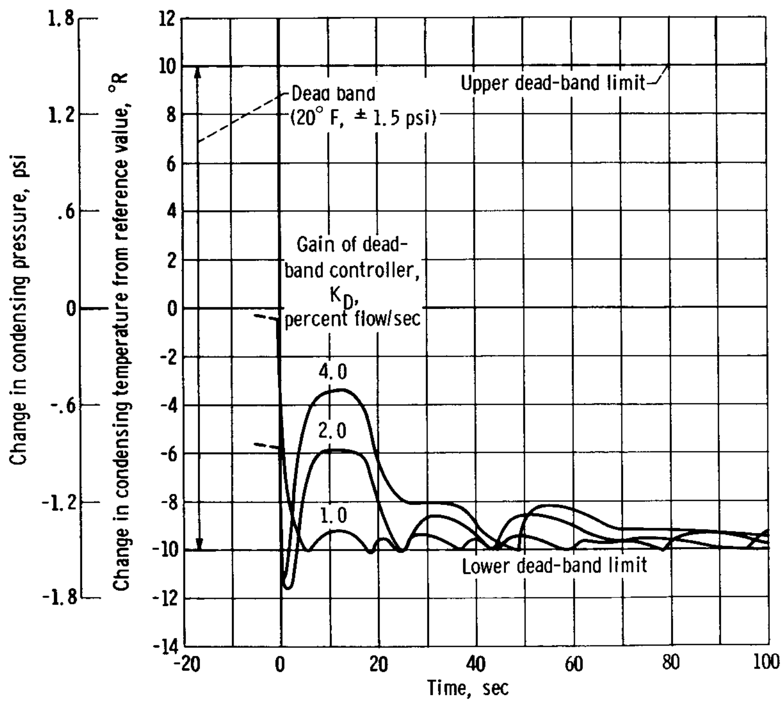

Figure 18. - Response of condensing temperature with dead-band control of condenser coolant bypass flow for stepdown in mercury flow rate.

and the oscillations are of lower frequency.

Figure 18 shows the step response of a flow control using a dead band and integral action. (The bypass valve position is changed at a constant rate as long as the error remains outside the dead-band limits.) Because of its complexity, no hand analysis was done for this mode. The step responses for the various indicated values of gain show, however, that this method of control could be implemented successfully. The gain K_D is the rate of change of flow rate (percent flow/sec).

The results of the investigation indicate that a stable, proportional control that manipulates condenser coolant bypass flow can be designed that will reduce the condensing temperature error due to various disturbances by a factor of about 5. The maximum bandwidth of the control system is limited to about 0.1 cps because of the condenser dynamics.

Comparison of Inventory Control and Flow Control

The conclusions of the dynamic investigation are condensed in the form of dynamic characteristics and are given in table II. As is shown in the table, the accumulator form

TABLE II. - SUMMARY OF DYNAMIC CHARACTERISTICS

Control	Stability	Speed of response	Steady-state error (offset), percent	Range of control	Control complexity	Acceleration sensitivity
Inventory control						
Accumulator inventory control	Good	Very fast	<3	Not limited	Very simple	Very high
Positive displacement inventory control	Good	Slow	Depends on type of control action	Not limited	Requires sensor, controller, power supply	None
Flow control						
Fast controller	Good	Fast	22	Not limited	Mildly complex	None
Slow controller	Good	Slow	28	Not limited	Mildly complex	None
Integral action	Good	Slow	<3	Not limited	Complex	None
Flow control with dead band	Good	Slow	Width of dead band	Not limited	Simple	None

of inventory control has the most rapid speed of response and can control the condensing pressure to small steady-state errors utilizing an extremely simple mechanization; however, it is very sensitive to acceleration, especially with a working fluid as dense as mercury. The more complex positive displacement variation on inventory control, while overcoming the acceleration sensitivity, would most likely decrease the speed of response.

The various forms of condenser bypass control, as shown in table II, are insensitive to acceleration; however, the control mechanization may be complex and exhibit some steady-state offset.

After consideration of the earlier mentioned criteria and of the need for ground testing under space-simulated conditions in order to flight rate the control system, condenser coolant bypass flow control with a constant radiator flow is considered to be the best choice for the SNAP-8 system. In addition to being insensitive to acceleration, it has the further advantage that it can be developed concurrent with and independent of the system up to and including the final system design and testing, at which time its actual need will have been experimentally determined. Finally, the speed of response is deemed adequate to handle transients which are anticipated in SNAP-8 space operation.

SUMMARY OF RESULTS

The expected variations of condensing pressure and methods for controlling these variations in the SNAP-8 Rankine space power system were investigated.

Condensing pressure, for a condenser operating with a radiator in a heat-rejection loop, was shown to be most sensitive to changes in power loop (mercury) flow rate, condenser inlet quality, radiator emissivity, and heat-rejection loop flow rate. Medium to low sensitivities were shown for space sink temperature, solar flux, radiator absorptivity, and condensing length.

Five modes of condensing pressure control were investigated. Four involved configuration changes in the heat-rejection loop to control flow rate and the fifth involved variation of condensing length (or inventory) by means of an accumulator. Steady-state studies showed that the most effective method of the first four schemes was to control condenser coolant flow by bypassing it around the condenser so as to maintain loop flow constant. The accumulator method was also an effective control method; however, a study of several design parameter variations showed that this method of control may require that the condenser be redesigned to have a more desirable characteristic.

Frequency response and transient behavior of the condenser coolant bypass and accumulator modes of control were analyzed and both were found adequate for the expected SNAP-8 disturbances.

The condenser coolant bypass control was finally recommended as the best choice because of insensitivity to acceleration (which permits adequate ground testing), severability at a late date in the development program if shown conclusively not to be needed, and compatibility with present system component operating characteristics.

Lewis Research Center,
National Aeronautics and Space Administration,
Cleveland, Ohio, June 10, 1966,
701-04-00-00-22.

REFERENCE

1. Schoenberg, Andrew A.: Mathematical Model with Experimental Verification for the Dynamic Behavior of a Single-Tube Condenser. NASA TN D-3453, 1966.